

A numerical model of the atmosphere of Venus

C. Lee *, S.R. Lewis, P.L. Read

Atmospheric Oceanic and Planetary Physics, Department of Physics, University of Oxford, Clarendon Laboratory, Parks Road, Oxford, Oxfordshire OX1 3PU, United Kingdom

Received 29 September 2004; received in revised form 18 March 2005; accepted 27 March 2005

Abstract

A new general circulation model (GCM) of Venus is being developed at Oxford. Venus presents unique numerical and physical challenges because of its thick atmosphere, slow underlying solid body rotation, and super-rotating atmosphere. Preliminary results from a GCM with simplified physical parameterizations are discussed. The current model uses linearized cooling and friction schemes, and spans five decades of pressure (0–90 km). The model is able to demonstrate significant global super-rotation, and although not yet fully realistic, future plans include more detailed representation of the Venusian atmosphere, such as the planetary boundary layer (PBL) scheme. The use of the model is discussed in supporting and interpreting data from future missions to Venus. © 2005 COSPAR. Published by Elsevier Ltd. All rights reserved.

Keywords: Venus; GCM; Super-rotation; Waves; Vortex

1. Introduction

Strong prograde zonal winds have been observed in the atmosphere of Venus, with peak velocities just above the cloudy regions, near 70 km altitude, of 100 ms^{-1} . The equatorial surface of the planet rotates at just 2 ms^{-1} (Schubert, 1983).

The cause of this super-rotation is not fully understood. From Hide (1969), it is clear that zonal mean processes alone cannot maintain a steady super-rotation, only re-distribute the angular momentum. Eddy processes are needed to maintain the observed super-rotation, as noted by Gierasch (1975).

A number of possible eddy processes which might maintain the super-rotation have been suggested, including tidal forcing (Gold and Soter, 1969), solar heating (Schubert and Whitehead, 1969) and orographic scattering (Fels, 1977). Previous models include those of Ros-

sow and Williams (1979) and Yamamoto and Takahashi (2003, 2004).

The current GCM uses simplified physical parameterizations to attempt to model the eddy processes using a flat “billiard ball” topography and no diurnal cycle. The linearized physical schemes used in the current model are similar to the Yamamoto and Takahashi (2003) model, except that Rayleigh (surface) friction is not used on potential temperature in this model.

The dynamical core of the model (which solves the meteorological primitive equations on a spherical grid) is based on the UK Meteorological Office Unified Model (Cullen, 1993). The present version of the model uses a 5° horizontal spacing and a maximum vertical level spacing of 3.5 km.

The radiative forcing and boundary layer parameterizations of the model are replaced with linear relaxation schemes, reflecting of the current lack of knowledge of detailed physics on Venus.

The radiative forcing in the model is replaced by a linear (Newtonian) cooling scheme as

* Corresponding author. Tel.: +44 186 527 2913; fax: +44 186 527 2923.

E-mail address: leec@atm.ox.ac.uk (C. Lee).

$$\frac{dT(\lambda, \phi, \eta, t)}{dt} = \frac{T_m(\lambda, \phi, \eta)}{\tau(\eta)} - \frac{T(\lambda, \phi, \eta, t)}{\tau(\eta)}, \quad (1)$$

where T is the temperature of the atmosphere, T_m is the state the atmosphere relaxes towards. ϕ , λ , and η are the latitude, longitude and pseudo-pressure coordinates of the model. τ is the relaxation timescale.

The fully relaxed state is formed from a global mean temperature profile based on the Pioneer Venus entry probe data (Seiff et al., 1980) and a cosine latitudinal gradient to simulate the effect of absorption of radiation in the cloud decks. The global mean temperature profile and the equator–pole temperature difference profile are shown in Fig. 1.

The boundary layer parameterization is replaced with a linear (Rayleigh) friction scheme on the lowest level only

$$\frac{d\vec{u}(\lambda, \phi, \eta, t)}{dt} = -\frac{\vec{u}(\lambda, \phi, \eta, t)}{\tau_R}, \quad (2)$$

where τ_R is the relaxation period; in this model $\tau_R = 32$ Earth days. \vec{u} is the horizontal velocity vector.

A ∇^6 diffusion is used to filter numerical noise and Rayleigh friction is applied to the zonally asymmetric components of the velocities on the top three layers to prevent spurious reflections from the model top.

The results shown here are for a model run started from rest, integrated for 18,000 Earth days and then sampled at 6-hourly intervals for 360 days. During this latter period, the globally averaged kinetic energy and potential energy vary by less than 5% and 1%, respectively.

2. The zonal mean state

The zonal mean zonal velocity and zonal mean temperature anomaly (i.e. the difference between the temperature at each point and the latitudinal mean

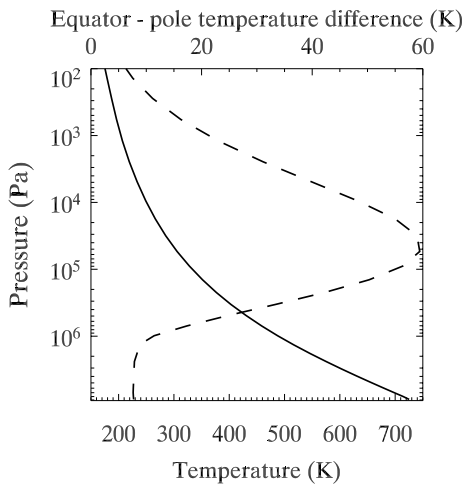


Fig. 1. (solid line) Global mean temperature profile (K). (dashed line) Equator–pole temperature difference (K).

temperature) for the atmosphere during this sampling period are shown in Figs. 2 and 3, respectively. The zonal mean zonal velocity has a peak of 45 ms^{-1} in the southern mid-latitudes and a small retrograde velocity near the surface. The atmosphere above 2 km is in prograde rotation relative to the surface.

The zonal mean zonal velocity of the atmosphere, shown in Fig. 2 is lower than the observed cloud-top wind speed of approximately 100 ms^{-1} and the winds calculated for retrieved temperatures assuming cyclostrophic balance (e.g. Del Genio and Rossow, 1990). The model does exhibit a significant super-rotation, but with a maximum zonal wind speed of about 60 ms^{-1} .

The latitudinal temperature anomaly of the atmosphere is shown in Fig. 3. The peak in temperature in the equatorial region (and corresponding trough near the pole) at 10^5 Pa is caused by the prescribed heating. There is also a reversal of the latitudinal temperature gradient near $5 \times 10^3 \text{ Pa}$, this reversal is not forced in

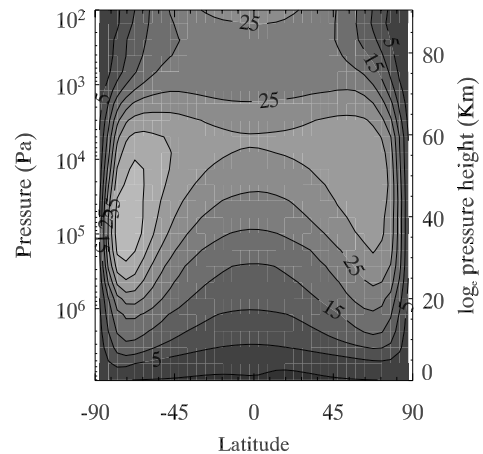


Fig. 2. Zonal mean zonal velocity (ms^{-1}). Contour separation is 5 ms^{-1} .

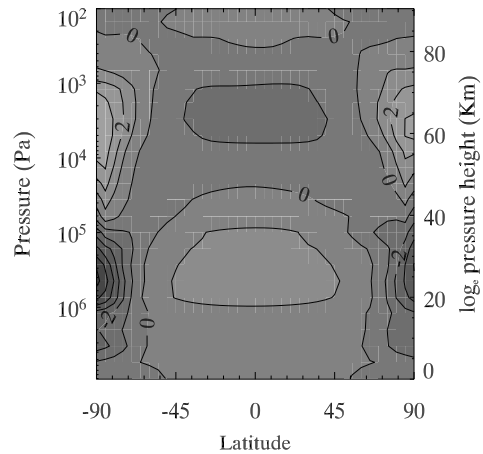


Fig. 3. Zonal mean temperature anomaly (K). Contour separation is 1 K.

the model but is related to the spontaneous tendency for the zonal jet closure at that height driven by the mean meridional circulation.

The reversal of the latitudinal temperature gradient with height was observed by the Pioneer Venus Orbiter Infra-Red Radiometer (Taylor et al., 1980), described as the ‘polar collar’ (which occurs in the region between the two extremes of the equator–pole gradient, at 5×10^4 Pa) and a polar bright spot (where the pole is warmer than the equator).

3. Atmospheric waves

Observations of waves in the atmosphere of Venus, reported by Del Genio and Rossow (1990) from UV cloud patterns, show two large scale modes. An equatorially trapped mode (with virtually no meridional velocity) is observed with a period of 3–5 Earth days and a mid-latitude Rossby-like wave with a period of 4–6 Earth days. The equatorial wave is normally the faster propagating wave mode.

The frequency spectra as a function of latitude are shown in Fig. 4. The figure shows the 95% confidence interval of a wave in temperature and meridional velocity having a given period. The spectra were obtained by Fourier decomposition of the data and comparing the power spectrum to a red noise spectrum derived from the lag-1 autocorrelation of the data.

The waves in the model atmosphere are dominated by two large scale wave modes. The first are equatorial Kelvin waves, with periods of 8–12 days. The second are mixed Rossby-gravity waves in the mid-latitudes, with periods of 15–25 days. The wave periods in the model do not closely match those observed, but would be consistent with Doppler shifted frequency relative to the

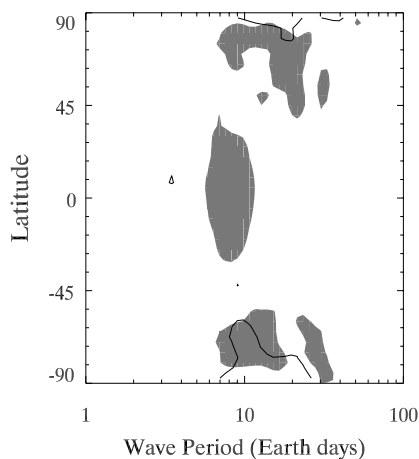


Fig. 4. Spectrum of waves in temperature (shaded region) and meridional velocity (line contour). Each region represents the 95% significance interval for a wave of given period and latitude.

zonal wind speed to match the observed cloud top winds. The model waves are qualitatively similar in latitude range and wave speed (e.g., relative to the zonal velocity) to those reported by Del Genio and Rossow (1990).

The wavenumber one equatorial Kelvin wave has a faster propagation speed than the zonal mean zonal velocity in the region where its amplitude is significant. The mid-latitude wave (also a wavenumber one) has a slower propagation speed than the zonal velocity.

The vertical structure of the equatorial waves suggests vertical propagation away from the peak latitudinal temperature gradient in Fig. 3 (both upwards and downwards), consistent with a deceleration of the zonal flow in this region.

4. Polar vortex

The polar vortex, discussed in Section 2 can also be seen in the longitude–latitude maps using data from the model. With the exception of the polar dipole observed inside the polar collar (Taylor et al., 1980), the model produces a similar structure to the observed polar features. Figs. 5 and 6 show the polar collar and bright-spot in the model atmosphere, separated by approximately 10 km in height. Pioneer Venus observations suggest the polar cold collar peaks at about 60 km and polar ‘bright spot’ peaks approximately 10 km above the polar collar.

The wave number one in the model extends over 50 km in the vertical and makes 1.5 complete loops of the pole in this height. Temperature isosurfaces of the

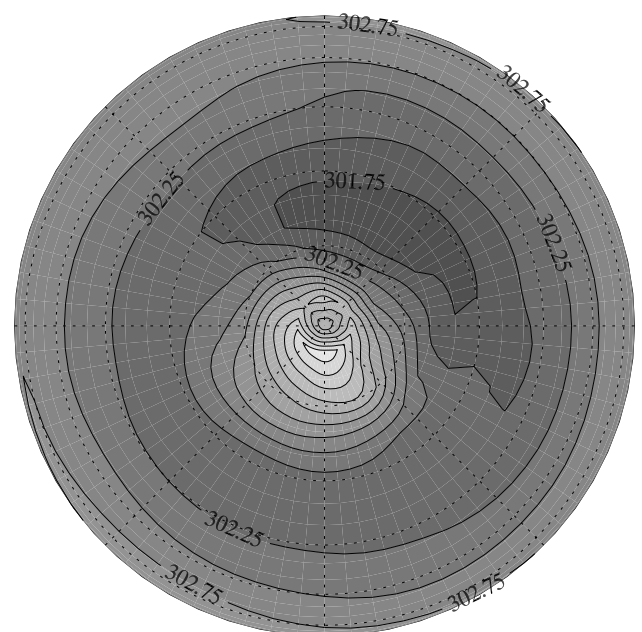


Fig. 5. Polar ‘cold collar’ at 600 hPa. Contour separation is 0.25 K.

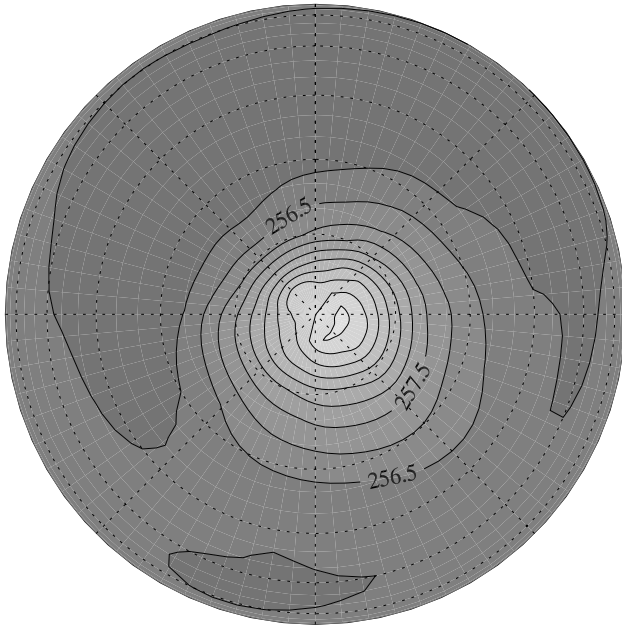


Fig. 6. Polar 'hot-spot' at 70 hPa, Contour separation is 0.5 K.

wave structure move equatorward with height and tilt backwards in longitude with height. This indicates significant baroclinic structure in the wave mode.

5. Conclusions

The GCM qualitatively produces a number of the significant features observed in the atmosphere of Venus, though quantitative agreement will require further tuning of the forcing processes. The model atmosphere super-rotates and reproduces the large scale waves observed by Del Genio and Rossow (1990) and the polar vortex observed by Taylor et al. (1980). The model also suggests a link between the mid-latitude waves and the polar vortex, in that both features exist in the model over similar height and latitude ranges.

Current development of the model is concentrated on the boundary layer region and a realistic surface topography for the model. This should allow surface effects such as stationary waves to be investigated.

The model can be used to assist with analysis and interpretation of Venus Express data such as interpreting a vertical structure from the cloud motion images captured by the Venus Monitoring Camera (Markiewicz et al., 2004). Data assimilation may allow temperature data from Venus Express to constrain and test the model or provide better parameterization data, as well as resulting in a self-consistent synoptic mapping of the data.

Acknowledgements

This work was funded by a PPARC studentship (C. Lee). Financial support for travel to the 35th COSPAR scientific assembly was provided to C. Lee by the ESA Education Department. The authors thank the UK Meteorological Office for the use of the HadAM climate model in this work.

References

- Cullen, M.J.P. The unified forecast/climate model. *Meteorol. Mag.* 122, 81–94, 1993.
- Del Genio, A.D., Rossow, W.B. Planetary-scale waves and the cyclic nature of cloud top dynamics on Venus. *J. Atmos. Sci.* 47, 293–318, 1990.
- Fels, S.B. Momentum and energy exchanges due to orographically scattered gravity waves. *J. Atmos. Sci.* 34, 499–514, 1977.
- Gierasch, P.J. Meridional circulation and the maintenance of the Venus atmospheric rotation. *J. Atmos. Sci.* 32, 1038–1044, 1975.
- Gold, T., Soter, S. Atmosphere tides and the 4-day circulation on Venus. *Icarus* 14, 16–20, 1969.
- Hide, R. Dynamics of the atmosphere of the major planets with an appendix on the viscous boundary layer at the rigid bounding surface of an electrically conduction fluid in the presence of a magnetic field. *J. Atmos. Sci.* 26, 841–853, 1969.
- Markiewicz, W.J., Titov, D., Keller, H.U., Jaumann, R., Michalik, H., Crisp, D., Esposito, L., Limaye, S.S., Watanabe, S., Ignatiev, N., Thomas, N. Venus monitoring camera for Venus Express. *Geophys. Res. Abs.*, 2004, 1607-7962/gra/EGU04-A-03942.
- Rossow, W.B., Williams, G.P. Large-scale motion in the Venus stratosphere. *J. Atmos. Sci.* 36, 377–389, 1979.
- Seiff, A., Kirk, D.B., Young, R.E., Blanchard, R.C., Findlay, J.T., Kelly, G.M., Sommer, S.C. Measurements of thermal structure and thermal contrasts in the atmosphere of Venus and related dynamics observations: results from the four Pioneer Venus probes. *J. Geophys. Res.* 85, 7903–7933, 1980.
- Schubert, G. General circulation and the dynamical state of the Venus atmosphere. in: Hunten, D.M., Colin, L., Donahue, T.M., Moroz, V.I. (Eds.), *Venus*. The University of Arizona Press, Tucson, pp. 681–765, 1983.
- Schubert, G., Whitehead, J.A. Moving flame experiment with liquid mercury: possible implications for the Venus atmosphere. *Science* 163, 71–72, 1969.
- Taylor, F.W., Beer, R., Chahine, M.T., Diner, D.J., Elson, L.S., Haskins, R.D., McCleese, D.J., Martonchik, J.V., Reichley, P.E., Bradley, S.P., Delderfield, J., Schofield, J.T., Farmer, C.B., Froidevaux, L., Leung, J., Coffey, M.T., Gille, J.C. Structure and meteorology of the middle atmosphere of Venus: infrared remote sensing from the Pioneer orbiter. *J. Geophys. Res.* 85, 7963–8006, 1980.
- Yamamoto, M., Takahashi, M. The fully developed super-rotation simulated by a general circulation model of Venus-like atmosphere. *J. Atmos. Sci.* 60, 561–574, 2003.
- Yamamoto, M., Takahashi, M. Dynamics of Venus' super-rotation: the eddy momentum transport processes newly found in a GCM. *Geophys. Res. Lett.* 31, L09701, 2004.